Gas Processing Journal

Vol. 7, No. 2, 2019, pp. 77-90
http://gpj.ui.ac.ir

DOI: http://dx.doi.org/10.22108/gpj.2020.115704.1049

Performance Evaluation of Series and Parallel Two-Stage Absorption Chillers Driven by Solar Energy: Energetic Viewpoint

Farshad Moradi Kashkooli [1], Mohsen Rezaeian [1], Mostafa Sefidgar [2*], Madjid Soltani [1], Mostafa Mafi [3]

[1] Department of Mechanical Engineering, K. N. Toosi University of Technology, Tehran, Iran
[2] Department of Mechanical Engineering, Pardis Branch, Islamic Azad University, Pardis, Iran
[3] Department of Mechanical Engineering, Imam Khomeini International University, Qazvin, Iran
Iran

Received: 2019-05-12 Revised: 2019-12-12 Accepted: 2020-01-04

Abstract: In recent years, the use of absorption chillers in air conditioning applications has increased in favor of less power consumption. Since absorption chillers require much less power compared to other common devices in the air conditioning industry, extensive efforts have been made in order to model, design, and optimize these systems. This study has investigated the effect of using solar energy on parallel and series two-stage refrigeration systems. First, both systems were designed, and then by connecting the solar collector to the absorption refrigeration system, the COP of the system and fuel consumption was calculated. Then, the impact of changing the evaporator's temperature on the system's COP was studied. The thermodynamic analysis of the system was conducted and the internal variables, such as pressure and temperature of different parts including the condenser and the evaporator, were calculated. Results indicate that the COP of the parallel cycle with a LiBr-H_2O working fluid is higher than that of a series cycle, so this leads to a significant drop in fuel consumption.

keywords: Absorption Chiller, Solar Energy, LiBr-H_2O Refrigerant, Absorption Refrigeration System

1. Introduction

Nowadays, a large number of refrigeration systems use mechanical compression that is energy-intensive. Nevertheless, there is a growing concern about conventional refrigeration system operating fluids which contribute to the destruction of the ozone layer, greenhouse effects, and global warming. Improvement of refrigeration systems more economically and more environmentally-friendly is one of the alternative options to tackle these challenges. Recently, there has been a growing attention in research to improve the absorption refrigeration systems (ARSs) (Kaynakli and Kilic, 2007). This system is a possible choice for using the remaining heat and renewable resources such as geothermal and solar energies (Soltani et al., 2019a, 2019b). The use of renewable and abundant solar radiation is suggested as an appropriate substitute. Recently, solar chillers may represent a suitable alternative for water and gas air conditioners, which consume electricity to a large extent. Moreover, the working fluids of these processes are compatible with the environment (Sun et al., 2012). Although the overall cooling effect per unit of supplied energy performance of the ARS is usually low, the remaining heat such as the one rejected from power plants may be used to increase the global energy utilization (McQuiston et al., 2004).

In the absorption refrigeration cycle, the required heat for the generator is supplied by solar energy. In order to run the working fluid in absorption chillers, thermal energy is used, which may be supplied through steam, hot water resulting from direct combustion of fuel, or through solar energy. Many researchers have worked on the double-effect H_2O-LiBr ARS by performing energy, exergy, and economic analyses (Kaushik and Arora, 2009; Kaynakli et al., 2015; Gomri, 2009; Talukdar and Gogoe, 2016, Morosuk and Tsatsaronis,

* Corresponding Author.
Authors' Email Address: [1] F. Moradi Kashkooli (farshadmoradikashkooli@ymail.com), [2] M. Rezaeian (mohsenrezaeeian@gmail.com), [3] M. Sefidgar (msefidgar@pardisiau.ac.ir), [4] M. Soltani (m.soltani@kntu.ac.ir), [5] M. Mafi (m.mafi@eng.ikiu.ac.ir), ISSN (Online): 2345-4172, ISSN (Print): 2322-3251

2008; Misra et al., 2005; Bereche et al., 2009). One main characteristic of the double-effect ARSs is its capability to work in parallel, series, and reverse parallel flow configurations with respect to the operating solution flow via the heat exchangers and generators (Arun et al., 2000, 2001; Garousi Farshi et al., 2011, 2012). Liu and Wang (2004) studied the performance of a LiBr-H_2O gas/solar double-effect ARS. In their intended system, the high-pressure generator is run by conventional energy, natural gas, and solar energy. Results indicated that this system is economically feasible and efficient. Molero-Villar et al. (2012) carried out a comparison between solar-powered ARSs to select the most appropriate condition of cooling systems containing solar energy. Boudéhenn et al. (2012) investigated the LiBr-H_2O absorption chiller system equipped with a solar energy collector. Sun et al. (2015) studied a gas/solar absorption cooling and heating system in a commercial building. Results indicated that 49.7% saving is achieved in the consumption of gas using this system. Mussati et al. (2018) investigated the configuration optimization of series flow double-effect LiBr-H_2O ARSs by minimizing the costs. Razmi et al. (2018) presented a system that works by hybridization of an ideal vapor compression system with a single-effect absorption system.

Performance analysis and thermodynamic modeling of ARSs are common in the study of vapor absorption cooling research. Performance of double-effect ARSs have been assessed in the literature (Garousi Farshi et al., 2011, 2012; Talpada and Ramana, 2019; Kaushik et al., 2018; Lima et al., 2019; Sioud et al., 2018). A comprehensive review of vapor ARSs and hybrid ARSs is performed for solar cooling applications by Kaushik et al. (Kaushik et al., 2018). The thermodynamic model developed for a prototype absorption chiller using NH_3/$LiNO_3$ is investigated by Lima et al. (2019). Recently, Sioud et al. (2018) investigated the feasibility and the eventual improvement in the performance of an ejector powered LiBr-H_2O double-effect absorption/recompression refrigeration cycle driven by high-temperature heat sources.

Given the high consumption of absorption chillers and the amount of power and energy required in the generator of the system, evaluating the savings in gas consumption by employing a solar collector, as an alternative solution, can be very useful and needs to be further investigated. The present study will address the effect of employing solar energy on fuel consumption of series and parallel two-stage ARSs. First, two intended systems are designed and then, the COPs of the refrigeration system and also power consumption are calculated by connecting the solar collector to the ARS. In the following, the impact of varying the evaporator temperature on the COP of the system will be studied. A thermodynamic analysis of the system is conducted and the internal variables such as pressure and temperature of different components including the condenser and the evaporator are calculated.

2. Mathematical Modeling

2.1. System Description

The main components of two-stage absorption chillers include evaporator, absorber, high-temperature generator (HTG), low-temperature generator (LTG), condenser, steam and liquid separator, high-temperature heat exchanger (HTHX), low-temperature heat exchanger (LTHX), low-temperature soluble pump, soluble pump, and refrigerant pump. In absorption cycles, the efficiency of refrigeration equipment is assessed using the COP. Figs. 1 and 2 respectively illustrate a schematic of the parallel and series double-effect absorption chillers with the absorber soluble of LiBr. These cycles have an evaporator, an HTG absorber, an LTG, two heat exchangers, and two condensers. In the series cycle, an outlet dilute soluble from the absorber is pumped into an LTHX, and is then let into an HTHX and afterward directly into a HTG. However, in the parallel cycle, this dilute soluble is injected into the LTG and the HTG simultaneously, the evaporated water enters the condensers and the concentrated soluble returns the absorber as in the series cycle. In both series and parallel cycles, the evaporated water taken from the LiBr-H_2O solution enters a distinct condenser in each generator.

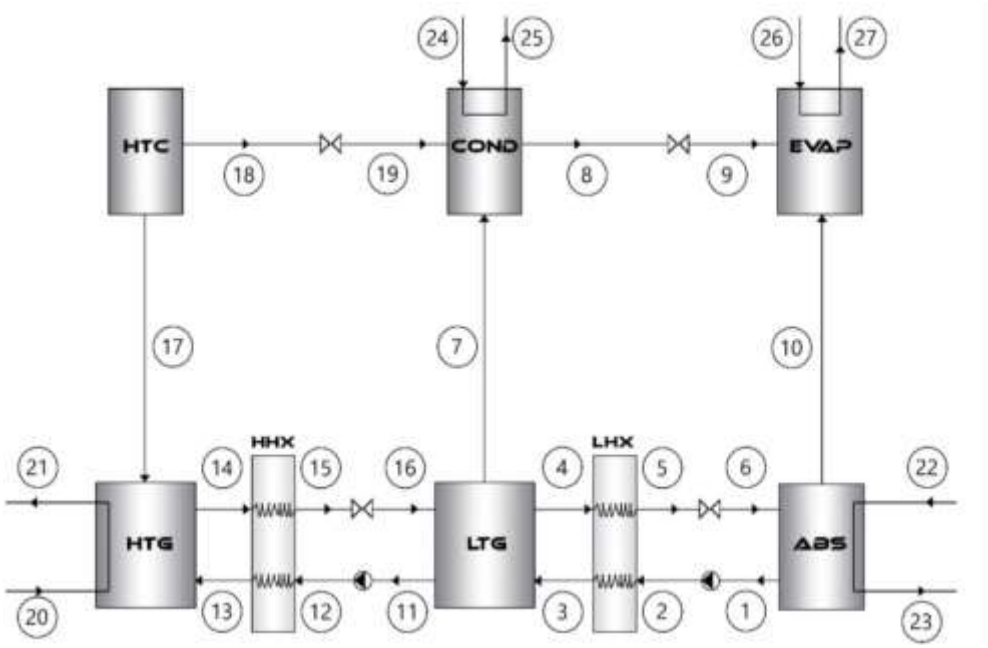

Figure 1. LiBr-H_2O double-effect cycle of the parallel type

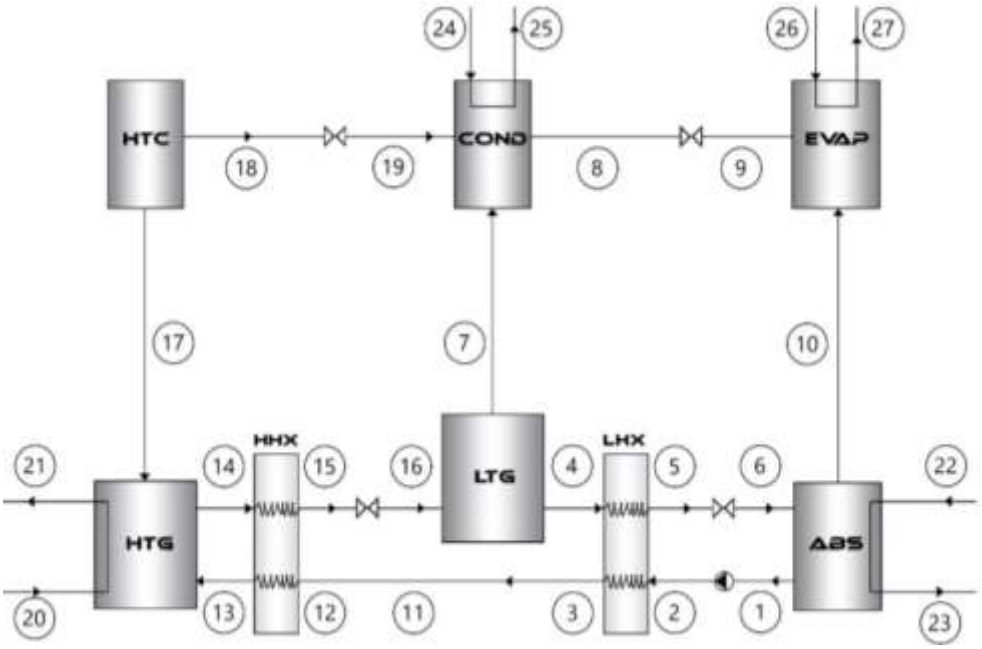

Figure 2. LiBr-H_2O double-effect cycle of the series type

The schematics of the modeled system are shown in Figs.1 and 2. The system is composed of two generators, one absorber, two condensers, one evaporator, two pumps, two expansion valves, and two heat exchangers. As demonstrated by Fig. 1, the system has five temperature values (for LTG, HTG, high-temperature condenser (HTC), condenser, and absorber), and three pressure levels (low pressure in the evaporator and the absorber, medium pressure in the condenser and LTG, and high pressure in HTG and HTC).

The term "double-effect" refers to the fact that the inlet heat is used twice in the cycle of vapor production at high temperatures. The generated vapor is used as the inlet heat in the HTG. This vapor, then, enters the high-temperature, where phase-change or condensation occurs due to loss of heat. This heat is high enough to move vapor out of the

heat exchanger in the LTG. Therefore, the heat is utilized twice and demonstrates double effects.

One of the main options of designing in double-effect technology for increasing the COP is the selection method of the flow connections. The major options for this case are the series and the parallel types of flows. The cycle demonstrated in Fig. 1 is drawn with the assumptions of parallel flow and also the same change in mass fraction of each generator. Fig. 2 illustrates a schematic of the series flow, where the flow in this direction first enters the HTG and then the LTG. In both cases, the process of internal heat exchange between the HTC and the LTG restricts the temperature. The HTC must have a high enough temperature for heat transfer to LTG.

2.2. System Modeling

The cycle has been modeled using the equations of energy and mass balance, for each component. The outlet mass flow rate of absorber is denoted by $\dot{m}_1$.In general, it is expected that the flow rate at the upper circuit (pump 2) be specified. Yet, the energy balance equation between the HTC and the low-temperature one is utilized to calculate the higher flow rate. The heat exchanger's mass flow rate is specified in four foreign heat transfer loops. As the initial temperature of each loop is specified, the value of U_a is assumed the input data for each of the external heat exchangers. This value is also considered for the condenser (U_{acd}). The assumptions and the considered inputs are similar to the parallel flow model.

2.2.1. Assumptions of the Problem

To model the double-effect of the ARS, several assumptions are considered as the following:

1- The system and the heat exchanger are under steady-state conditions.

2- At the condenser outlet, water is a saturated liquid.

3- At the evaporator outlet, water is a saturated vapor.

4- LiBr's temperature at the absorber outlet is the absorber's temperature.

5- The outlet heat temperature of the absorber and the generator depends on the balance conditions of mixing and separation.

6- Heat loss and pressure drop in the tubes and heat exchangers have been ignored.

7- Heat exchange between the system and the environment does not occur except in the HPG, the evaporator, the condenser, and the absorber.

8- In default conditions of system, water is operated with a temperature of 25 ℃ and pressure of 1 atm.

2.3. Thermodynamic Analysis

The equations and the first and second laws of thermodynamics are taken into consideration in this section. The first law of thermodynamics defines energy transfer, while the second law describes the quality of energy and material. In order to conduct thermodynamic analysis of the ARS, the mass equation, and the first and second laws of thermodynamics have been applied to each component of the system equipment.

Mass equations including the mass balance governing the whole cycle and conservation of concentration equation under steady-state flow and steady-state system conditions are as follows:

$$\sum \dot{m}_i = \sum \dot{m}_o \tag{1}$$

$$\sum \dot{m}_i X_i = \sum \dot{m}_o X_o \tag{2}$$

where ṁ and X denote mass flow rate and mass concentration of LiBr, respectively. These equations are written for chiller components of the parallel and series cycles.

The first law of thermodynamics demonstrates the energy balance equation for each component, and it is stated as follows:

$$\sum \dot{m}_i h_i - \sum \dot{m}_o h_o) + (\sum Q_i - \sum Q_o) + W = 0 \tag{3}$$

where Q denotes the value of the heat transfer between the control volume of system and its surrounding environment, and W is the positive work amount of system. Energy balance for components of these systems in parallel double-effect conditions is presented as Table 1. It is noteworthy that the equations of the double-effect series system components are also similar to these equations.

The overall performance of energy in refrigeration cycles is demonstrated using the COP, which is defined as follows:

$$COP_{chiller} = \frac{Q_{eva}}{Q_{gh} + W_p} \tag{4}$$

In this study, EES software version 9.4 was used for data analysis and sensitivity analysis. Conducting the calculations related to the first and second laws of thermodynamics, thermal efficiency, component equations, and other

thermodynamic and mathematical calculations are achieved by programming in EES.

Table 1. Energy balance equations for different components in double-effect series and parallel systems

Equations	Components
$Q_{gh} = \dot{m}_{17} \cdot h_{17} + \dot{m}_{14} \cdot h_{14} - \dot{m}_{13} \cdot h_{13}$	
$Q_{gh} = \dot{m}_{20} \cdot cp(h_{21} - h_{20})$	
$lmtd_{gh} = \frac{T_{20} - T_{14} - (T_{21} - T_{17})}{ln[\frac{T_{20} - T_{14}}{T_{21} - T_{17}}]}$	HTG
$UA_{gh} = \frac{Q_{gh}}{lmtd_{gh}}$	
$Eff_{LHX} = \frac{T_4 - T_5}{T_4 - T_2}$	
$Q_{LHX} = \dot{m}_1 \cdot (h_3 - h_2)$	
$Q_{LHx} = \dot{m}_4 \cdot (h_4 - h_5)$	
$lmtd_{LHX} = \frac{T_4 - T_3 - (T_5 - T_2)}{ln[\frac{T_4 - T_3}{T_5 - T_2}]}$	LTHX
$UA_{LHX} = \frac{Q_{LHX}}{lmtd_{LHX}}$	
$Eff_{HHX} = \frac{T_{14} - T_{15}}{T_{14} - T_{12}}$	
$Q_{HHx} = \dot{m}_{11} \cdot (h_{13} - h_{12})$	
$Q_{HHx} = \dot{m}_{14} \cdot (h_{14} - h_{15})$	
$lmtd_{HHX} = \frac{T_{14} - T_{13} - (T_{15} - T_{12})}{ln[\frac{T_{14} - T_{13}}{T_{15} - T_{12}}]}$	HTHX
$UA_{HHX} = \frac{Q_{HHX}}{lmtd_{HHX}}$	
$Q_{HTC} = \dot{m}_{17} \cdot (h_{17} - h_{18})$	
$lmtd_{HTC} = \frac{T_{18} - T_4 - (T_{18} - T_{16})}{ln[\frac{T_{18} - T_4}{T_{18} - T_{16}}]}$	HTC
$UA_{HTC} = \frac{Q_{HTC}}{lmtd_{HTC}}$	
$Q_{cd,in} = \dot{m}_7 \cdot h_7 + \dot{m}_{19} \cdot h_{19} - \dot{m}_8 \cdot h_8$	
$Q_{cd,out} = \dot{m}_{24} \cdot cp(T_{25} - T_{24})$	
$lmtd_{cd} = \frac{T_8 - T_{24} - (T_8 - T_{25})}{ln[\frac{T_8 - T_{24}}{T_8 - T_{25}}]}$	Condenser
$UA_{cd} = \frac{Q_{cd}}{lmtd_{cd}}$	
$Q_{eva} = \dot{m}_9 \cdot (h_{10} - h_9)$	
$Q_{eva} = \dot{m}_{27} \cdot cp(T_{26} - T_{27})$	
$lmtd_{eva} = \frac{T_{26} - T_{10} - (T_{27} - T_9)}{ln[\frac{T_{26} - T_{10}}{T_{27} - T_9}]}$	Evaporator
$UA_{eva} = \frac{Q_{eva}}{lmtd_{eva}}$	
$\dot{m}_{10} \cdot h_{10} + \dot{m}_6 \cdot h_6 - Q_{abs} - \dot{m}_1 \cdot h_1 = 0$	
$Q_{abs} = \dot{m}_{22} \cdot cp(T_{23} - T_{22})$	
$lmtd_{abs} = \frac{T_6 - T_{23} - (T_1 - T_{22})}{ln[\frac{T_6 - T_{23}}{T_1 - T_{22}}]}$	Absorber
$UA_{abs} = \frac{Q_{abs}}{lmtd_{abs}}$	
$\dot{m}_3 \cdot h_3 + \dot{m}_{16} \cdot h_{16} + \dot{m}_{17} \cdot h_{17} = \dot{m}_4 \cdot h_4 + \dot{m}_{11} \cdot h_{11} + \dot{m}_{18} \cdot h_{18} + \dot{m}_7 \cdot h_7$	LTG and HTC

3. Results and Discussion

This section analyzes and compares the results obtained from the simulation. After presenting the obtained results and sensitivity analysis of different parameters, the best-operating conditions are selected for the system. First, to examine the accuracy of the calculations, the results of the present simulation for the COP have been compared with the work of Gomri (2009) in Fig. 3. The results of this comparison have indicated a completely desirable match between the two studies. Results of the simulation including the system's thermodynamic properties are shown for the series and parallel cycles in Table 2. Other specifications including the system's COP, the pump's power consumption, the heat transfer rate of each component, and the heat exchanger's efficiency are presented in Table 3.

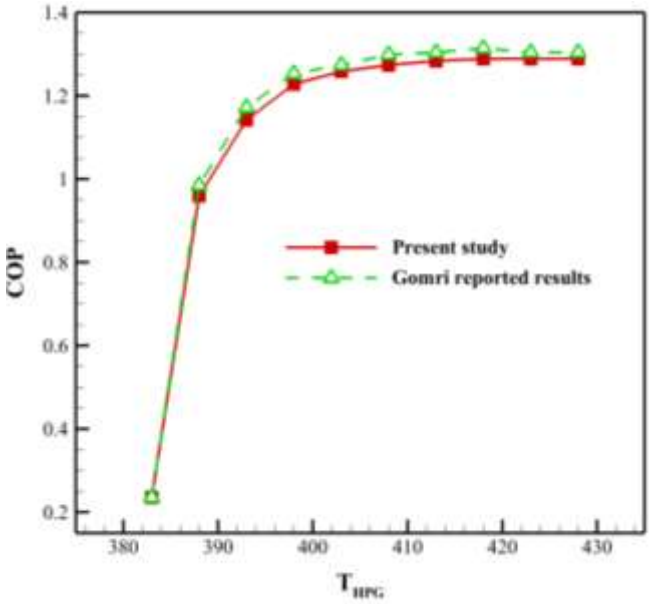

Figure 3. Verification of the results of the current study with the study of Gomri (2009) for the conditions of T_{con}=360K & T_{eva}=277K

Table 2. Thermodynamic specifications of the parallel and series flow cycles

Parallel flow						Series flow					
Point	T (℃)	ṁ (kg/s)	X (%)	h (J/g)	s (J/g K)	Point	T (℃)	ṁ (kg/s)	X (%)	h (J/g)	s (J/g K)
1	29.78	1.00	52.613	65.0	0.203	1	29.89	1	52.839	65.9	0.2029
2	29.78	1.00	52.613	65.0	0.203	2	29.89	1	52.839	65.9	0.2029
3	54.41	1.00	52.613	117.5	0.366	3	57.45	1	52.839	124.4	0.3844
4	76.81	0.85	61.921	195.6	0.427	4	78.98	0.844	62.615	203	0.434
5	43.89	0.85	61.921	133.9	0.244	5	44.62	0.844	62.615	139.3	0.2461
6	47.29	0.85	61.921	133.9	0.264	6	48.38	0.844	62.615	139.3	0.2675
7	57.69	0.067	0	2,607.6	8.613	7	58.66	0.074	0	2,609.4	8.605
8	30.14	0.15	0	126.2	0.4384	8	30.63	0.156	0	128.3	0.4453
9	5.3	0.15	0	126.2	9.016	9	5.05	0.156	0	128.3	9.022
10	5.3	0.15	0	2,510.3	9.016	10	5.04	0.156	0	2,509.8	9.022
11	57.69	0.55	52.613	124.5	0.387	11	-	-	-	-	-
12	57.71	0.55	52.613	124.5	0.388	12	-	-	-	-	-
13	103.47	0.55	52.613	222.4	0.664	13	107.46	1	52.839	231.1	0.6842
14	145.42	0.46	61.921	324.3	0.765	14	140.29	0.918	57.554	304.5	0.7965
15	84.02	0.46	61.921	209.1	0.465	15	82.3	0.918	57.554	188.3	0.4917
16	77.45	0.46	61.921	209.1	0.430	16	69.11	0.918	57.554	188.3	0.4165
17	123.17	0.08	0	2,725.9	7.683	17	129.68	0.082	0	2,737.4	7.619
18	88.31	0.08	0	369.8	1.173	18	93.68	0.082	0	392.4	1.235
19	30.14	0.083	0	369.8	1.242	19	30.63	0.082	0	392.4	1.315
20	150.00	8,000	0	2,746.4	6.838	20	150.00	8	0	2,746.4	6.838

21	142.40	8,000	0	599.6	1.764	21	141.88	8	0	597.3	1.759
22	25.00	12,000	0	104.8	0.367	22	25.00	12	0	104.8	0.367
23	33.45	12,000	0	140.1	0.4839	23	33.80	12	0	141.6	0.4886
24	25.00	12,000	0	104.8	0.367	24	25.00	12	0	104.8	0.367
25	28.72	12,000	0	120.3	0.418	25	29.08	12	0	121.8	0.4238
26	12.00	20,000	0	50.4	0.180	26	12.00	20	0	50.4	0.1804
27	7.73	20,000	0	32.5	0.117	27	7.57	20	0	31.8	0.1149

The assumption in this system is that the maximum mass ratio must be smaller than the point where crystallization occurs because this occurrence is not desired for the system. In other words, this requirement is an assumption made to simplify the modeling.

In the following, by changing the absorber's outlet flow rate, variations in the value of the system's COP may be observed for both cycles. Fig. 4 presents the variations in COP versus the absorber outlet flow rate. The COP of the parallel flow is higher than the series flow; however, the reduction of the system's COP by increasing the absorber's outlet mass flow rate is similar in both of the cycles. On the other hand, although the COP of the series flow cycle is smaller than that of the parallel flow, it is of higher capacity.

Table 3. Specifications of different components of the cycle in both the parallel and the series flows

Parameter	Parallel flow	Series flow	Unit
COP	1.404	1.363	-
Eff_{LHX}	70	70	%
Eff_{HHX}	70	70	%
UA_{LHX}	2.923	3.266	[kW/K]
UA_{HHX}	1.61	3.723	[kW/K]
UA_{eva}	85	85	[kW/K]
UA_{abs}	50	50	[kW/K]
UA_{cd}	65	65	[kW/K]
UA_{HTC}	10	10	[kW/K]
UA_{HTG}	25	25	[kW/K]
$Q_{cd,,in}$	195.263	192.109	[kW]
Q_{abs}	426.059	443.517	[kW]
$Q_{cd,out}$	187.566	205.742	[kW]
Q_{eva}	358.386	371.708	[kW]
Q_{HTG}	225.215	272.719	[kW]
Q_{LHX}	52.429	58.511	[kW]
Q_{HHX}	53.971	106.715	[kW]
Q_{Tot}	1,713	1,843	[kW]
$W_{Pump\ 1}$	0.002	0.002	[kW]
$W_{Pump\ 2}$	0.022	-	[kW]

The overall heat transfer value has been investigated in Fig.5. This figure studies variations of the overall heat transfer with respect to the absorber's outlet flow rate for both of the series and the parallel flows. As the results demonstrate, it may be observed that an increase in the overall exchanged heat in terms of the absorber's outlet flow rate is not linear, and the increasing slope is decreased at higher flow rates.

The results of Fig.6 indicate that the COP is better in the parallel cycle than in series one. As is observed, with an assumption of 280 K temperature for the evaporator, the COP of the parallel cycle is always higher at all temperature levels of the high-pressure generator than that of the series cycle. Furthermore, it was observed at other temperature levels considered for the evaporator that increasing the temperature in the high-pressure generator results in increasing COP. However, the rate of increase in COP at initial temperatures of the high-pressure generator (range of 390-420 K) was higher, and as the temperature increases (range of 420-470 K), the rate of increase in COP reduces. The parallel cycle has consistently shown a better performance than the series cycle.

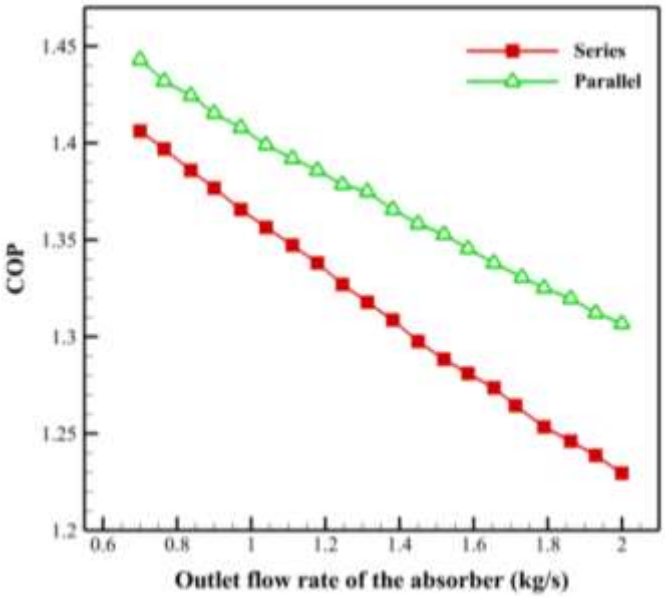

Figure 4. Variations in COP in terms of the outlet flow rate of the absorber

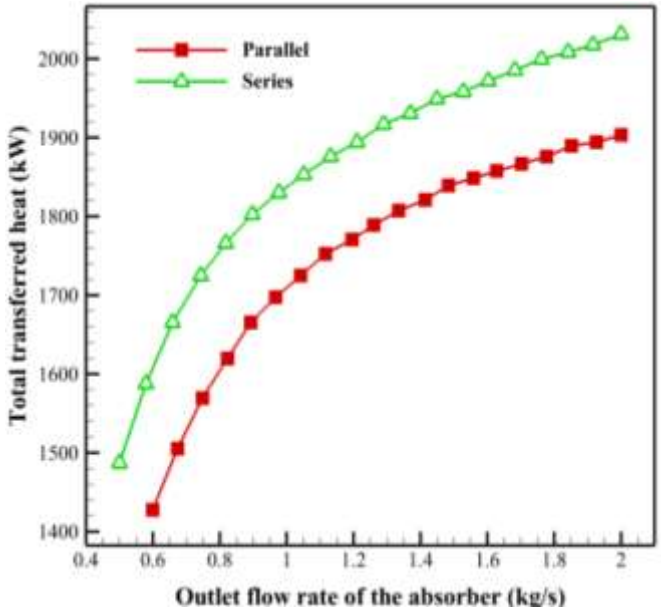

Figure 5. The amount of total exchanged heat with respect to the absorber's outlet flow rate

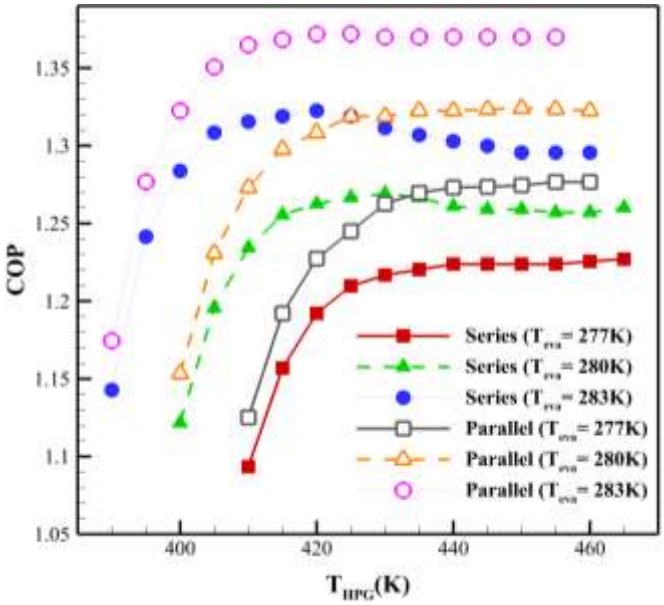

Figure 6. The effect of the evaporator's and the generator's temperatures on COP

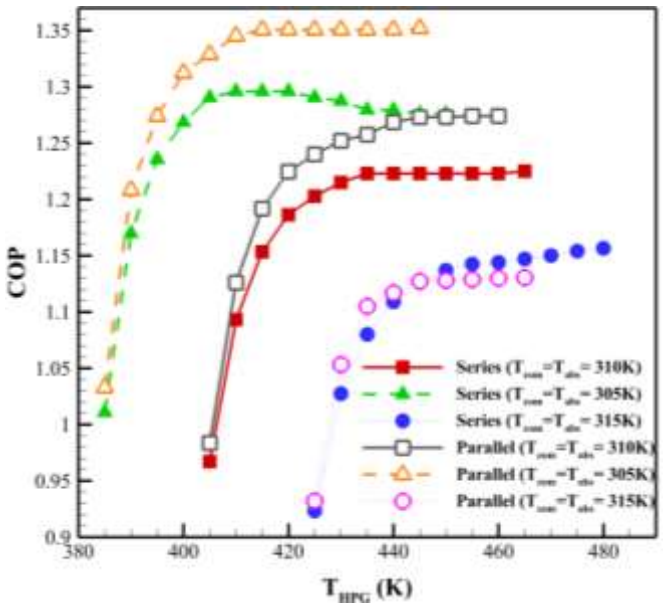

Figure 7. The impact of the condenser's and the generator's temperatures on COP

Fig. 7 shows variations of the cycle's COP with respect to the variations in the temperature of the condenser as well as the generator's temperature on the cycle. Results demonstrated the superiority of the parallel cycle's COP to the series one.

In Fig.8, other parameters including the evaporator and the generator's temperature variations to the pressure have been investigated. It may be observed that pressure variations in the series cycle are intensively increasing, while such variations in the parallel cycle are insignificant compared to the series cycle. This shows that the parallel cycle is more reliable than series one.

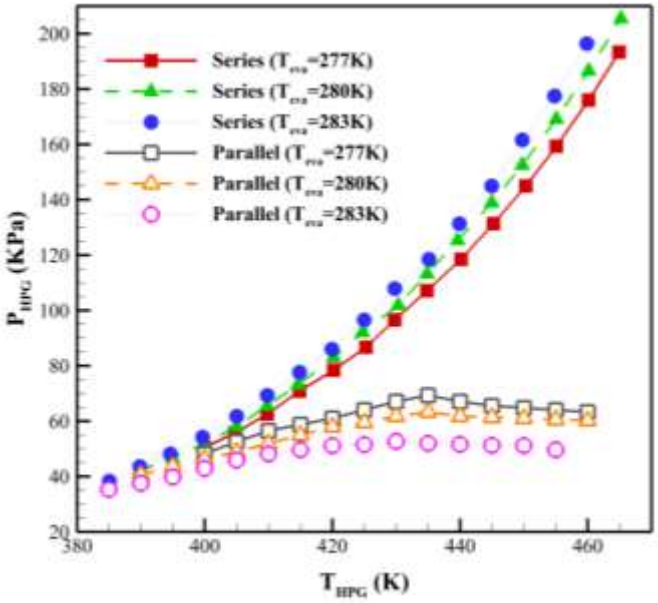

Figure 8. The impact of the evaporator's and the generator's temperatures on the pressure of the high-pressure generator

Fig.9 provides investigation of variations in the generator's pressure by changing the temperature of the condenser and the generator. As is observed, with an increase in the condenser's temperature in the parallel cycle, variations of pressure at various temperatures are different but insignificant. However, in the series cycle, such variations are almost equal at different temperatures, but pressure variations are intensively increased.

It may be observed in Fig.10 that increasing the efficiency of high-and LTHXs would change COP in the series and the parallel cycles. With an increase in the efficiency of HTHX, the parallel cycle COP is higher than that of the series. Also, in LTHX, with an increase in efficiency, the parallel cycle COP is higher than that of the series. This fact, by itself, indicates the superiority of the parallel cycle to the series one with respect to efficiency in HTHX and LTHXs.

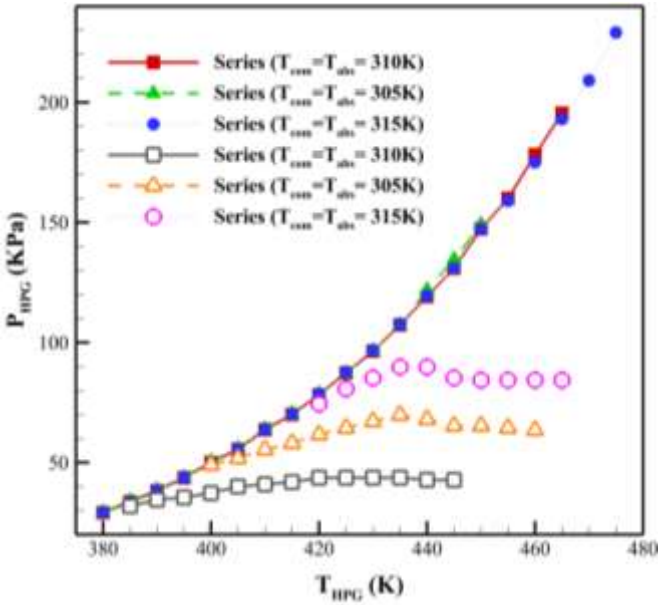

Figure 9. The impact of the condenser's and the generator's temperatures on the pressure of HPG

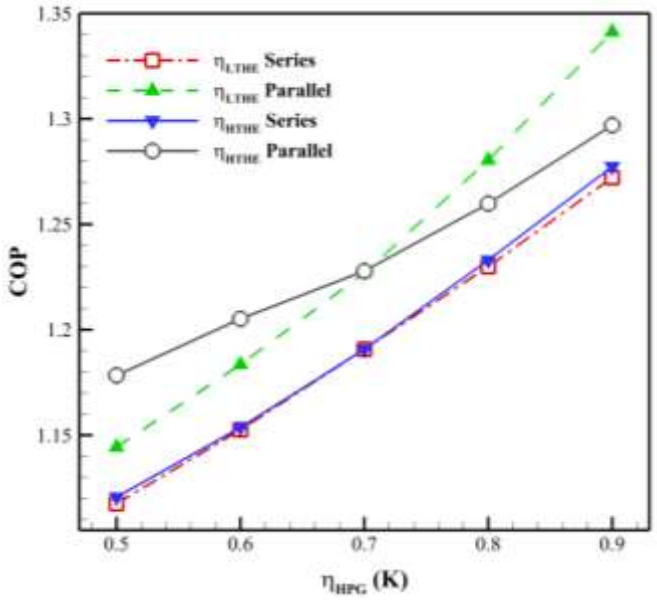

Figure 10. The effect of HTHE and LTHXs on COP

6. Conclusion

The purpose of examining two parallel and series cycles in the present study is the optimization of the system. In refrigeration cycles, unlike in other cycles, the capability of the system's performance is studied through COP. It should be noted that this procedure is similar in water-ammonia fluid, and only the working fluid changes. On the other hand, the efficiency and COP of LiBr systems are always greater than those of ammonia. Therefore, to optimize the system, different comparisons have been made between the series and the parallel cycles by analyzing the LiBr-H_2O system. Results demonstrated that the parallel cycle with LiBr-H_2O working fluid has a higher COP than the series cycle. Thus, the proposed LiBr-H_2O parallel cycle model may be utilized in order to optimize the system. The inlet heat source in the present work is supplied by solar energy, which is assumed as an inlet heat source with a specified flow rate and temperature in the results and analyses. This value may be reduced or increased to optimize consumption in the system with the best COP, the fact which is directly related to fuel consumption. In other words, considering different uses and applications, temperatures, and conditions, these assumptions may vary. Thus, the amount of fuel consumption or the energy source will also change. In conclusion, it may be stated that the performance of the first and the second laws of thermodynamics of the parallel cycle is better than that of the series. As a result, this leads to a reduction of fuel consumption significantly. Furthermore, the parallel cycle with the mentioned conditions is efficient due to having the best COP and performance. The heat transfer in the evaporator, the absorber, the condenser, HTG, HTHX, and LTHX is lower in the parallel cycle than in the series one. However, in the parallel cycle, the heat transfer for the HTC is higher than that of the series cycle.

Nomenclature

ARS	Absorption refrigeration systems
COP	Coefficient of performance
Eff	Efficiency
HTC	High temperature condenser
HTG	High-temperature generator
HTHX	High-temperature heat exchanger
h	Enthalpy (J/g)
LTG	Low-temperature generator
LTHX	Low-temperature heat exchanger
$\dot{m}$	Mass flow rate (kg/s)
Q	Heat transfer (kJ)
S	Entropy (J/g K)
T	Temperature (K or ℃)
W	System positive work (kW)
X	Mass concentration (%)
Subscript	
abs	Absolute
com	Compressor
eva	Evaporator
i	Inlet
o	Outlet
Tot	Total

References

Arun, M.B., Maiya, M.P., & Murthy S.S. (2000) Equilibrium low pressure generator temperatures for double-effect series flow absorption refrigeration systems. *Applied Thermal Engineering*, 20, 227-242.

Arun, M.B., Maiya, M.P., & Murthy S.S. (2001) Performance comparison of double-effect parallel flow and series flow water–lithium bromide absorption systems. *Applied Thermal Engineering*, 21, 1273-1279.

Bereche, R.P., Palomino, R.G., & Nebra, S.A (2009) Thermoeconomic analysis of a single and double-effect LiBr/H_2O absorption refrigeration system. *International Journal of Thermodynamics*, 12, 89–96.

Boudéhenn, F., Demasles, H., W., J. (2012) Development of a 5 kW cooling capacity ammonia-water absorption chiller for solar cooling applications. *Energy Procedia,* 30, 35-43.

GarousiFarshi, L., Seyed Mahmoudi, S.M., & Rosen, M.A. (2011) Analysis of crystallization risk in double effect absorption refrigeration systems. *Applied Thermal Engineering*, 31, 1712–1717.

Garousi Farshi, L., Seyed, M., Rosen, M.A., & Yari, M.A. (2012) comparative study of the performance characteristics of double-effect absorption refrigeration systems. *International Journal of Energy Research*, 36, 182–92.

Gomri, R. (2009) Second law comparison of single effect and double effect vapour absorption refrigeration systems. *Energy Conversion and Management*, 50, 1279–1287.

Liu, Y.L. & Wang, R.Z. (2004) Performance prediction of a solar/gas driving double effect LiBr-H_2O absorption system. *Renewable Energy*, 29(10), 1677-1695.

McQuiston, F.C., Parker, J.D., & Spitler, J.D. (2004) Heating, ventilating and air conditioning analysis and design. 6th ed. Hoboken, NJ: Wiley.

Misra, R.D., Sahoo, P.K., & Gupta, A. (2005) Thermoeconomic evaluation and optimization of a double-effect H_2O/LiBrvapour-absorption refrigeration system. *International Journal of Refrigeration*, 28, 331-343.

Morosuk, T. & Tsatsaronis, G. A (2008) new approach to the exergy analysis of absorption refrigeration machines. *Energy*, 33, 890-907.

Morosuk, T. & Tsatsaronis, G. (2009) Advanced exergetic evaluation of refrigeration machines using different working fluids. *Energy*, 34, 2248-58.

Molero-Villar, N., Cejudo-López, J.M., & Domínguez-Muñoz, F. (2012) A comparison of solar absorption system configurations. *Solar Energy*, 86(1), 242-252.

Mussati, S. F., Cignitti, S., Mansouri, S. S., Gernaey, K.V., Morosuk, T., & Mussati, M.C. (2018) Configuration optimization of series flow double-effect water-lithium bromide absorption refrigeration systems by cost minimization. *Energy Conversion and Management*, 158, 359-372.

Kaynakli, O., & Kilic, M. (2007) Theoretical study on the effect of operating conditions on performance of absorption refrigeration system. *Energy Conversion and Management*, 48, 599-607.

Kaushik, S.C., & Arora, A. (2009) Energy and exergy analysis of single effect and series flow double effect water–lithium bromide absorption refrigeration systems. *International Journal of Refrigeration*, 32, 1247-1258.

Kaushik, S.C., Arora, A., &Dixit, M. (2018) Hybrid absorption cycles for solar cooling. Hybrid absorption cycles for solar cooling. In: Zhang G., Kaushika N., Kaushik S., Tomar R. (eds) Advances in Energy and Built Environment. Lecture Notes in Civil Engineering, vol. 36. Springer, Singapore, 2018.

Kaynakli, O., Saka, K., &Kaynakli, F. (2015) Energy and exergy analysis of a double effect absorption refrigeration system based on different heat sources. *Energy Conversion and Management*, 106, 21-30.

Lima, A.A.S., Ochoa, A.A.V., da Costa, J.Â.P., dos Santos, C.A.C., Lima, M.V.F., &de Menezes, F.D. (2019) Energetic analysis of an absorption chiller using NH_3/$LiNO_3$as an alternative working fluid. *Brazilian Journal of Chemical Engineering*, 36, 1061-1073.

Razmi, A., Soltani, M., M. Kashkooli, F., &G. Farshi, L. (2018) Energy and exergy analysis of an environmentally-friendly hybrid absorption/ recompression refrigeration system. *Energy Conversion and Management*, 164, 59-69.

Sioud, S.F., Cignitti, S., Mansouri, S.S., Gernaey, K.V., Morosuk, T., & Mussati, M.C. (2018) Configuration optimization of series flow double-effect water-lithium bromide absorption refrigeration systems by cost minimization. *Energy Conversion and Management*, 158, 359-372.

Soltani, M., M. Kashkooli, F., Dehghani-Sanij, A.R., Kazemi, A.R., Bordbar, N., Farshchi, M.J., Elmi, M., Gharali, K., & Dusseault, M. B. (2019a) A comprehensive study of geothermal heating and cooling systems. *Sustainable Cities and Society*, 44,793-818.

Soltani, M., M. Kashkooli, F., Dehghani-Sanij, A.R, Nokhosteen, A., Ahmadi-Joughi, A., Mahbaz, S.B., & Dusseault, M. B. (2019b) A comprehensive review of geothermal energy evolution and development. *International Journal of Green Energy*, 16(13), 971-1009.

Sun, J., Fu, L., &Zhang, S. (2012) A review of working fluids of absorption cycles. *Renewable & Sustainable Energy Reviews*, 16, 1899-1906.

Sun, H.Q., Xu, Zh. Y., Wang, H.B., & Wang, R. Zh. (2015) A Solar/gas Fired Absorption System for Cooling and Heating in a Commercial Building. *Energy Procedia*, 70, 518-528,

Talpada, J.S., & Ramana P.V. (2019)A review on performance improvement of an absorption refrigeration system by modification of basic cycle. *International Journal of Ambient Energy*, 40, 661-673.

Talukdar, K., & Gogoi, T.K. (2016) Exergy analysis of a combined vapor power cycle and boiler flue gas driven double effect water–LiBr absorption refrigeration system. *Energy Conversion and Management*, 108, 468-477.